Rev Bras Cir Cardiovasc 2011;26(2):155-63

Fractal dimension in quantifying the degree of myocardial cellular rejection after cardiac transplantation

Dimensão fractal na quantificação do grau de rejeição celular miocárdica pós-transplante cardíaco

Roberto Douglas MOREIRA[1], Antonio Roberto MORIEL[2], Luiz Otávio MURTA JUNIOR[3], Leandro Alves NEVES[4], Moacir Fernandes de GODOY[5]

RBCCV 44205-1262

Abstract

Introduction: **The term "Fractal" is derived from the Latin fractus meaning "irregular" or "broken" considering the observed structure with a non-integer dimension. There are many studies which employed the Fractal Dimension (FD) as a diagnostic tool. One of the most common methods for its study is the "Box Counting Method".**

Objective: **The aim of the present study was to try to establish the contribution of FD in the quantification of myocardial cellular rejection after cardiac transplantation.**

Methods: **Microscopic digital images were captured at 800x600 resolution (magnification 100x). FD was calculated with the aid of "ImageJ software" with adaptations. The classification of the degrees of rejection was in agreement with the "International Society for Heart and Lung Transplantation" (ISHLT 2004). The final report of the degree of rejection was confirmed and redefined after an exhaustive review of the slides by an external experienced pathologist. 658 slides were evaluated with the following distribution among the degrees of rejection (R): 335 (0R); 214 (1R); 70 (2R); 39 (3R). The data were statistically analyzed with Kruskal-Wallis tests and ROC curves being considered significant values of *P* d" 0.05.**

Results: **There was significant statistical difference between the various degrees of rejection with the exception of R3 versus R2. The same trend was observed in applying the ROC curve.**

Conclusion: **FD may contribute to the assessment of myocardial cellular rejection. Higher values are directly associated with progressively higher degrees of rejection. This may help in decision making of doubtful cases and those which contemplate the intensification of immunosuppressive medication.**

Descriptors: **Cardiac surgical procedures. Graft rejection. Heart transplantation. Biopsy.**

Resumo

Introdução: **O termo "fractal" é derivado do latim *fractus*, que significa "irregular" ou "quebrado", considerando a estrutura observada como tendo uma dimensão não-inteira. Há muitos estudos que empregaram a Dimensão Fractal**

1. Specialist Physician in Cardiology at Federal Council of Medicine; Collaborator Professor at São José do Rio Preto Medical School (FAMERP), São José do Rio Preto, SP, Brazil.
2. Pathologist Physician at Brazilian Society of Pathology; Pathologist Physician at Pathology and Cytopathology Anatomy of São José do Rio Preto, SP, Brazil.
3. PhD in Physics; Head of the Computing and Mathematics Department at USP of Ribeirão Preto, SP, Brazil.
4. São Paulo State University, DEMAC, Rio Claro, SP, Brazil.
5. Full Professor in Cardiology at FAMPERP; Adjunct Director of Education at FAMPERP, São José do Rio Preto, SP, Brazil.

This study was carried out at São José do Rio Preto Medical School, FAMERP, São José do Rio Preto, SP, Brazil.

Correspondence address:
Moacir Fernandes de Godoy. Rua Garabed Karabashian, 570 – Mansur Daud – São José do Rio Preto, SP, Brazil – Zip Code: 15070-600.
E-mail: mfgodoy@netsite.com.br

Article received on February 14th, 2011
Article accepted on March 8th, 2011

(DF) como uma ferramenta de diagnóstico. Um dos métodos mais comuns para o seu estudo é a "*Box-plot counting*" (Método de contagem de caixas).

***Objetivo:* O objetivo do estudo foi tentar estabelecer a contribuição da DF na quantificação da rejeição celular miocárdica após o transplante cardíaco.**

***Métodos:* Imagens microscópicas digitalizadas foram capturadas na resolução 800x600 (aumento de 100x). A DF foi calculada com auxílio do "*software* ImageJ", com adaptações. A classificação dos graus de rejeição foi de acordo com a "Sociedade Internacional de Transplante Cardíaco e Pulmonar" (ISHLT 2004). O relatório final do grau de rejeição foi confirmado e redefinido após exaustiva revisão das lâminas por um patologista experiente externo. No total, 658 lâminas foram avaliadas, com a seguinte distribuição entre os graus de rejeição (R): 335 (0R), 214 (1R), 70 (2R), 39 (3R). Os dados foram analisados estatisticamente com os testes Kruskal-Wallis e curvas ROC sendo considerados significantes valores de $P \leq 0,05$.**

***Resultados:* Houve diferença estatística significativa entre os diferentes graus de rejeição com exceção da 3R *versus* 2R. A mesma tendência foi observada na aplicação da curva ROC.**

***Conclusão:* A DF pode contribuir para a avaliação da rejeição celular do miocárdio. Os valores mais elevados estiveram diretamente associados com graus progressivamente maiores de rejeição. Isso pode ajudar na tomada de decisão em casos duvidosos e naqueles que possam necessitar de intensificação da medicação imunossupressora.**

***Descritores:* Fractais. Rejeição de Enxerto. Transplante de Coração. Biópsia.**

INTRODUCTION

The current surgical methods for heart implants are primarily designed to allow the extension of life, and although the technical, surgical, scientific, social and ethical difficulties have been largely overcome, it should be emphasized the problem of rejection, which is an important factor which can limit the lifetime of the graft and, consequently, the long-term success [1,2].

The hyperacute rejection is an unusual form of rejection. It occurs as a causal factor to the presence of preformed cytotoxic antibodies in the recipient against antigens of the donor. It is characterized by sudden and irreversible dysfunction of the graft from minutes to hours after revascularization, with thrombotic occlusion of the microvasculature, the following neutrophil infiltration and hemorrhage in the myocardium [3].

The acute cellular rejection is the leading cause of morbidity and mortality between 30 days and 12 months post-transplant, along with chronic rejection and malignancies, is also a major cause of death in the late post-transplant. During the first year after transplantation, the incidence of acute rejection is situated around 40 episodes of rejection per 100 patients per month [4].

Acute rejection is characterized by vascular damage to the microcirculation, usually mediated by antibodies, whose specificity is not fully elucidated. T lymphocytes may also contribute. The main morphological substrate is the deposition of immunoglobulins and complement in the microcirculation, associated with vasculitis or endothelial swelling. Although some authors have reported high incidence, the rejection of vascular complications has not been considered routine in most centers [3].

Chronic rejection or graft vascular disease represents a major complication and is the main limiting factor of survival in late stage of the transplant. The graft vascular disease is responsible for most deaths in late post-transplant follow-up and its incidence reaches estimated values of 10% per year postoperatively, reaching 40-50% in recipients who complete the fifth year of follow-up [5].

The study of cardiac rejection after transplantation is very important for proper treatment of patients. Currently, this procedure is performed using endomyocardial biopsy (EMB) - serial or motivated by the clinical presentation. Concern for the rejection is so important that several methods for assessment have been proposed, like the biochemical markers and echocardiography. However, this event could still not be adequately predict and therefore further research with this approach should be encouraged.

The diagnosis of rejection after cardiac transplantation lies primarily on histopathological evaluation of endomyocardial biopsies, since the functional changes due to rejection are expressed in general later. Histological assessment of EMB, however, presents problems of sensitivity and does not always allow the distinction between mild episodes of rejection, self-limited, and those who will progress to more serious paintings. In this way, research on other methods that alone or in conjunction with the histological evaluation of endomyocardial biopsies, may contribute to greater accuracy in the

diagnosis of cardiac transplant rejection becomes of great importance [4].

Over the years, several methods have been proposed for the histological grading of cardiac rejection. The levels proposed in Workformulation WF 90 of International Society for Heart & Lung Transplantation (ISHLT) were based primarily on the amount of inflammatory infiltrate and the presence of myocyte damage. In 1990, Billingham et al. [6] at Stanford University, representing the Study Group on Cardiac Rejection of the ISHLT, published a formulation for the standardization of nomenclature in the diagnosis of heart and lung rejection.

This formulation has undergone a review in 2003 [7] and in 2004, a multidisciplinary working group, composed of international experts in cardiac transplantation, met in order to review the definitions of the classification of 1990 in terms of cellular rejection and antibody-mediated, in addition to identify areas of difficulty in the interpretation of post-transplant biopsies, and finally reviewing the grading system. There was a strong consensus that any change in the wording should reflect the current pathological practice and should not affect the gradation of historical samples. So the question was not exactly a change in the grading scale in 1990, but a way to define more clearly how pathologists and cardiologists should interpret the grading system.

Table 1 provides a comparison between the classification of 1990 and the amendments proposed in 2004.

Fractal Geometry

If a segment is measured using a measuring element that has r length equal to 1/3 of that line segment, three elements will obviously be necessary to overlap completely and that that segment will be valid for any chosen fraction, infinitely. Mathematically, the amount of information necessary to override this line segment is given by 1/r. If we now try to overlap a square of *1* side with small squares with *r* side in length, if each small square has r side, 0.5 value, then four squares will be necessary and mathematically this quantity can be obtained by formulating $1/r^2$. Finally, if we use small cubes to fill completely the volume of a cube of $1 \times 1 \times 1$, and if each *r* side of the small cubes, for example, measure 0.5, eight units will be required. Alternatively, if each *r* side measuring 1/3 (as usually seen in those puzzle called Rubik's Cube), then 27 units will be needed, ie, regardless of the *r* value, in the case of filling a cube will always be necessary $1/r^3$ units.

Recalling that in the case of superposition of a square with several small squares, the amount was expected to overlap $1/r^2$ and to overlap a line segment with several short segments was $1/r$. So, it is clear that the exponent, specifically for those structures considered, it is always

Chart1. Comparison between staging systems of acute cellular rejection in 1990 and 2004 classifications of the International Society for Heart and Lung Transplantation (ISHLT).

1990	2004
Grade 0 (no acute rejection)	Grau 0R (no acute rejection)
Grade 1A (focal mild acute rejection)	
Grade 1B (diffuse mild acute rejection)	Grau 1R (mild acute cellular rejection, low grade): interstitial infiltrate and/or perivascular up to 1 focus of myocyte damage.
Grade 2 (focal moderate acute rejection)	
Grade 3A (multifocal moderate acute rejection)	Grau 2R (acute cellular rejection, moderate, intermediate grade): 2 or more foci of infiltrate with associated myocyte damage
Grade 3B (diffuse severe borderline acute rejection)	Grau 3R acute cellular rejection, severe, high-grade): diffuse infiltrate with multifocal myocyte damage with or without edema, hemorrhage, or vasculitis.
Grade 4 (severe acute rejection)	

the same as the dimension of the object we are trying to overlap or fill, or, in the case of a straight, two in the case of the square and three in the case of cube.

For a generic formulation, then we have:

$$N_r = r^{-D} \text{ [Equation 1]}$$

where N_r is the number of equal elements necessary to overlap or fill in the original object, being *r* the ruler or scale applied to the object and *D* the size of that structure or object.

So far we have been dealing with so-called regular structures that obey the Euclidean geometry. In these structures, the size of the measured object is always the same, regardless of size or scale of the ruler used. The great majority of the nature structures, however, are called "fractals".

The neologism "Fractal" derives from the Latin adjective fractus, which means "irregular" or "broken", serving to indicate that the observed object or structure has an integer size, and may take values like 1.75 or 1.3492621 , for example. Then, it was opened with it, a chance for study and application of fractal geometry.

The "Fractal Geometry" was first introduced by Richardson (citation Karperien et al., 2008) [8] in 1960 to describe the coastlines. Richardson found that, depending on the scale used to measure a coastline, the total length obtained could vary. More specifically speaking, a decrease in the scale could eventually result in a non-linear increase in length. This finding was popularized by Benoit Mandelbrot, resulting in what today is called the fractal analysis, widely applied in various branches of science.

The mathematical manipulation of Equation 1 provides the solution to obtain what is known as fractal dimension, presented in Equation 2 below:

$$DF = \lim_{r \to 0} (\text{Log Nr} / \log r^{-1})$$

In the case of histological slides, there are several techniques for determining the fractal dimension. Among them, the Box-counting technique is one of the most used. In this technique, it is used the overlay image with squares of r side progressively smaller and in this case, Nr is the number of squares with r side needed to cover the image, in every size chosen. The FD is then the slope of the regression line of the two log-values, ie, the size of r side and the amount of Nr square [8]. The medical literature contains several studies that use fractal dimension as a diagnostic tool. Thus, the fractal dimension has been used to study neurons and glial cells, retinal ganglion cells, bone cells, histopathology of malignancies, renal and pulmonary vasculature, morphometry of hepatocytes, liver fibrosis and DNA structure, among many others [9.10].

METHODS

All endomyocardial biopsies were performed at the same service and myocardial fragments were obtained with the aid of specific bioptome. The bioptome was introduced preferably by jugular vein and, exceptionally, the right femoral vein or left jugular. Fragments of myocardium (usually three) were fixed in formalin 10% buffered and processed by paraffin embedding method. The sections were stained with hematoxylin-eosin (H&E). All this processing was performed in the same Clinical Pathology Service.

Microscopic images were digitally captured using the Olympus BX41 Trinocular Microscopic with *panchromatic* len of 10x coupled to a color digital camera Samsung SCC-131, U-adapter Olympus TV1X-2 at 800x600 resolution (100 x total increase) and saved in "jpeg" files.

In light of the new classification of degrees of rejection used in this study, according to the system recommended by the ISHLT [11], the initial report of each case was reviewed and the conclusive opinion on the degree of rejection was confirmed or redefined after thorough reevaluation of slides by an experienced pathologist (ARM), supported by further opinions when doubt justified them. In total, 658 slides were assessed with the following distribution between degrees of rejection: 335 (0R), 214 (1R) 70 (2R), 39 (3R).

The fractal dimension was estimated by Box-counting method, using the software ImageJ from the National Institute of Health (NIH), widely used in the literature and available free on the Internet (http://rsbweb.nih.gov/ij/). This software considers the Box-counting in two dimensions, allowing the quantification of the distribution of pixels harvest area, not considering, therefore, the texture image. The influence of this is that two images with the same distribution of pixels, and another in a binarized gray levels, possess the same fractal dimension. For this, the FD will be calculated with the ImageJ always between 0 and 2, not distinguishing different textures. The program received further implementation of the physicist and engineer LOMJ with plugins that facilitated the collection of results as a whole, including the possibility of simultaneous study of the Shannon Entropy and Counting of Cell Nuclei.

Statistical analysis was performed using the Stats Direct software version 2,7,2. It was performed the descriptive statistics and for comparison between groups 0R, 1R, 2R and 3R, we used the nonparametric statistical test of Kruskal-Wallis. In case of detection of overall statistical difference it was performed comparison between groups by the method Dwass-Steel-Chritchlow-Fligne test. The results are also presented graphically in box-plot format, and have been added yet calculations of sensitivity, specificity, positive predictive value, negative predictive value and accuracy, complementing the presentation of the

ROC curves with their respective areas under the curve. It was assumed an alpha error of 5% and were considered significant the *P* values less than or equal to 0.05.

The study was submitted to the Ethics Committee on Human Research of the institution, under protocol number 403/2007, on 12/17/2007.

RESULTS

The descriptive statistics of the fractal dimension values in different degrees of rejection is presented in Table 1.

Figure 1 shows the Box-plot graphs of the distribution of fractal dimension values of the degree of rejection of 0, 1, 2 and 3. There is a tendency that the higher levels of cardiac rejection are related to higher values of fractal dimension.

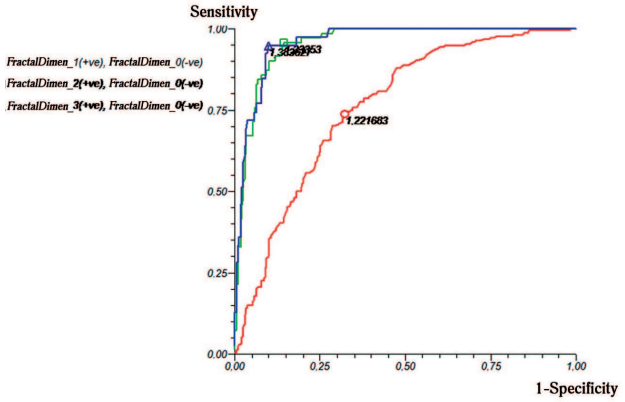

Fig. 2 - Graph of ROC curve for differentiation by fractal dimension between different degrees of cardiac rejection (grade 3 versus 0, Grade 2 vs. 0, grade 1 vs 0)

Table 1. Descriptive statistics of the values of fractal dimension in different degrees of rejection (grades 0, 1, 2 and 3).

Variable	Rejection Grade 0	Rejection Grade 1	Rejection Grade 2	Rejection Grade 3
No. Images	335	214	70	39
Mean	1.1795	1.3178	1.5396	1.5512
Standard Deviation	0.1529	0.1431	0.1175	0.1194
Maximum	1.6890	1.6969	1.7406	1.7279
Upper quartile	1.2556	1.4041	1.6273	1.6499
Median	1.1626	1.3026	1.5609	1.5808
Lower quartile	1.0830	1.2143	1.4639	1.4545
Minimum	0.8360	0.8833	1.2325	1.2459
Variation coefficient	0.1298	0.1085	0.0763	0.0769

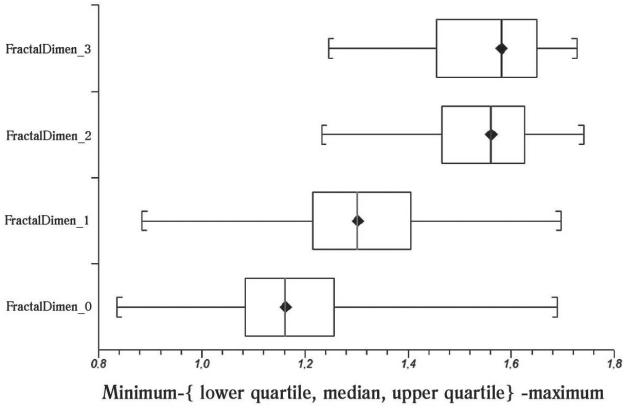

Fig. 1 - Box-plot graph (minimum, lower quartile, median, upper quartile, maximum values) of the fractal dimension of the sheets of endomyocardial biopsy, in different degrees of cardiac rejection

Statistical analysis by the non-parametric Kruskal-Wallis test shows the existence of a statistically significant difference between groups (P <0.0001).

The intergroup comparison method Dwass-Steel-Chritchlow-Fligne test shows significant difference (P <0.0001) for all combinations, except for Group 3R versus Group 2R (P = 0.9592).

Figure 2 shows that the best discrimination was obtained to differentiate between grade 2 versus grade 0 and between grade 3 versus grade 0, with areas under the curve, respectively, 0.9560 (95% CI 0.9199 to 0.9922) and 0.9594 (95% CI 0.9127 to 1.0000).

As for the distinction between grade 1 versus 0, the area under the curve was less pronounced, although still considered moderately high, with 0.7608 (95% CI 0.7177 to 0.8040).

Table 2. Sensitivity, specificity, positive predictive value and negative predictive value in differentiation between various degrees of rejection (grade 3 vs. 0, grade 2 versus 0, Grade 1 and Grade 0 versus 3 versus 2) according to the cutoff levels for Fractal Dimension.

	Grade 3 Versus 0	Grade 2 Versus 0	Grade 1 Versus 0	Grade 3 Versus 2
Cutt-off value	1.3836	1.3335	1.2216	1.6643
Sensitivity	0.9487	0.9571	0.7383	0.2307
Specificity	0.9014	0.8567	0.6776	0.8857
Positive predictive value	0.5286	0.5826	0.5940	0.5294
Negative predictive value	0.9934	0.9896	0.8022	0.6739

In differentiating between grades 3 versus 2, the area under the curve was 0.5289 (95% CI 0.4104 to 0.6474) and there is therefore, separation of groups 3 and 2 in terms of Fractal Dimension.

The cutoff levels for the different comparisons were:

- Group 3R versus 0R: greater than or equal to 1.3836;
- Group 2R versus 0R: greater than or equal to 1.3335;
- Group 1R versus 0R: greater than or equal to 1.2216;
- Group 3R versus 2R: greater than or equal to 1.6643.

The sensitivity, specificity, positive predictive value and negative predictive value of different cutoff levels in the separation between the groups are in Table 2.

Following, some illustrative cases of different histological features and their values of fractal dimensions within each degree of cardiac rejection are presented (Figure 3).

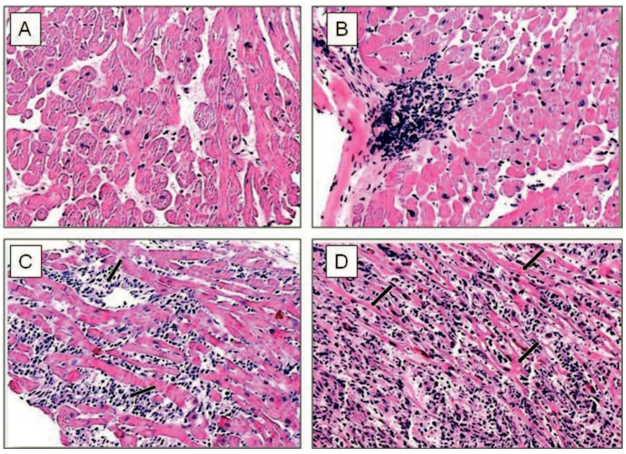

Fig. 3 - Photomicrographs of endomyocardial biopsies (Hematoxylin-eosin 100x), showing the myocardial fibers in Panel A in cross section (in the center-left) and longitudinal (near right) with preserved architecture and space with no signs of interstitial inflammatory infiltrate. Absence of rejection (Grade 0R). Fractal Dimension = 1.109; Panel B, the central left, single focus of mononuclear aggressive infiltrate, subendocardial, with involvement of myocytes, destruction and erasure of regional architecture. Mild acute cellular rejection (grade 1R). Fractal Dimension = 1.370, Panel C with moderate mononuclear cells and multiple foci of aggression to the myocytes (arrows), leading to destruction and widening of interstitial spaces, moderate acute cellular rejection (grade 2R). Fractal Dimension = 1.460, Panel D with changes in architecture by intense diffuse mononuclear inflammatory infiltrate, aggressive, with massive destruction of myocytes. Note some residual fibers in longitudinal section (arrows) marked by the inflammatory process, severe acute cellular rejection (Grade 3R). Fractal dimension = 1.670

DISCUSSION

The distribution of lymphocytes infiltrating the heart tissue is directly proportional to the standard histological classification (0R, 1R, 2R and 3R), which suggests that the distribution of these cells has a fractal dimension feature, which may be related to lymphocyte migration. In fact, the CD4 and CD8 T lymphocytes infiltrate the tissues during the inflammatory process of rejection as a result of stimulation by specific activation mechanisms mediated by antigenic differences between donor and recipient [12]. In addition, levels of proinflammatory cytokines that influence the receiver expresses the intensity of rejection and graft survival rate.

The facts reported above justify the progressive increase of fractal dimension documented in this study, since the amount of inflammatory cells also appeared in a growing and statistically significant rate.

The fractal dimension of the object counts the number of effective degrees of freedom in the dynamic system and thus quantifies its complexity. Thus, it appears that images with increased fractal dimension are therefore more complex. That was actually realized in the present study, in which images without rejection appeared in the visual impression less complexicity then images with rejection. One should not, however, only by the visual aspect, to quantify this complexity. The fractal dimension would then remedy this difficulty by adding an objective numerical value.

Kido et al. [13] assessed the fractal dimension of interstitial lung abnormalities in chest X-rays. One method used was the Box-counting. 100 regions of interest compared radiographs of 50 patients with interstitial pulmonary abnormalities and compared with 100 regions of interest in X-rays of 50 patients with normal lungs. The fractal dimension obtained in cases with interstitial disease was significantly higher when compared to normal lungs (1.67 ± 0.10 versus 1.44 ± 0.12, respectively, P <0.001).

Wielgus et al. [9] assessed the fractal dimension of the terminal villi of placentas of mature female smokers and nonsmokers during the third trimester of pregnancy. The placentas were obtained from 60 healthy women, primiparous women who had not received hormonal treatment and who were aged between 18 and 27 years. Three groups were studied: nonsmokers, smokers up to 30 cigarettes per day and smokers of more than 30 cigarettes per day. One method used to quantify the fractal dimension was the Box-counting. The results led to the conclusion that the fractal dimension obtained with this technique, regardless of several factors, allows to estimate the degree of density of placental terminal villi. Here, the density meant the ratio between the surface of the villi and the surface of the preparation assessed. They found also that the fractal dimension increased in direct relation to the number of

cigarettes smoked during pregnancy, although in both groups of women smokers fractal dimension was significantly lower than in the case of non-smokers (1.295 ± 0.021, 1.36 ± 0.009, 0.012 ± 1.63, respectively).

Vasilescu et al. [14] assessed the fractal dimension in the diagnostic differentiation between types of gastric carcinoma. They used, among others, the Box-counting technique that was considered by them the most appropriate technique. They compared the fractal dimension of the interface between the epithelial tissue and malignant tissue support (stroma), seeking to relate the fractal dimension of this region with the degree of invasiveness of the tumor. In their study they included 20 cases of gastric carcinoma and two cases of normal gastric tissue. The cancer group was divided into two subgroups: those with the so-called intestinal form and those with the diffuse form.

The intestinal form has a structure defined with glandular cells that resemble intestinal cancer, and less invasive. The diffuse type is composed of single cells or small clusters of cells that infiltrate the gastric wall layers. They found that lower values of fractal dimension were significantly associated with increased tumor invasiveness, ie, the fractal dimension of the epithelial-stromal interface was much smaller for the diffuse type of gastric carcinoma. The mean values and standard deviation for the normal gastric mucosa, intestinal type of gastric carcinoma and the diffuse type were, respectively, 1.622 ± 0.0667, and 1.5045 ± 0.0865 1.1711 ± 0.0799. The authors concluded that carcinogenesis would then be characterized by a loss of complexity and loss of self-similarity.

Dioguardi et al. [10] scanned sections of liver biopsies from 209 patients with hepatitis C and with different degrees of fibrosis or cirrhosis and analyzed, among others, the fractal dimension by box-counting method. They obtained fractal dimension values ranging from 1.22 to 1.79 and the value of this parameter increased depending on the extent of fibrosis, with the high *r* coefficient of 0.81. They concluded that increasing the fractal dimension, in this case, was due to disruption of the natural harmonic state, creating disorder in the normal lobular structure of liver tissue.

Sullivan et al. [15] performed a study to determine if the fractal analysis could be an appropriate method to measure migration of cell lines of human breast cancer. To this end, they compared the migration of MDA-MB-231 cells that have high mobility and the migration of invasive MDA-MB-468 cells of more moderate behavior in an experiment of tissue healing. They found that the intensity fluctuation of fractal dimension could be used as a tool for quantifying cell migration in terms of the severity of the cancer and treatment response. The fractal dimension has allowed a quantitative description of this cell migration.

Tambasco et al. [16] in 2009 assessed the material included in 82 paraffin blocks consisting of prostate tissue removed by needle biopsy from 82 different patients, 63 prostate tissue containing benign prostate tissue and 19 with carcinomas of high grade (Gleason 8 to 10). For each case, they prepared two blades, one being stained with hematoxylin-eosin and the other with Pan-keratin, which stains specifically epithelial structures. They used the measure of fractal dimension by box-counting method with housing widths ranging from a minimum of 4 microns (nominal size of the nucleus) to 340 microns (nominal size structure of a prostate gland).

This is relevant because this variation corresponds to the physical limits of the structure studied and, beyond these limits, the graphics start to deviate from linearity, since it does not contain more structural information, since there would be approach of the limit of resolution or pixel minimum size or, on the other end, there would reach a size larger than the largest structure in the image (500 microns). They observed that the differences between the average fractal dimension of prostate tissue compared to normal prostate tissue in high-grade tumor were significant (P <0.0001), with both HE staining and staining with Pan-keratin, but in the group stained with pan-keratin, the separation between the interquartile range, in units of fractal dimension, was higher than in group stained with HE (0.09 versus 0.01, respectively).

The fractal dimension of benign tissue was 1.85 ± 0.04 with HE staining and 1.51 ± 0.08 with Pan-keratin staining. Similarly, the fractal dimension of highly tumor tissue was 1.90 ± 0.04 with HE staining and 1.73 ± 0.09 with Pan-keratin staining. These differences are due to the fact that Pan-keratin is a more specific staining for glandular tissue, there were fewer structures stained than with HE, which have broader spectrum of action, staining more histological structures.

This highlights the importance of staining used. In our study we used only the HE staining, then opening up space for a revaluation of all the material with the possible use of other stainings.

The degree of brightness at which the images are obtained could possibly be in a bias, since it is virtually impossible to get all the slides with the same degree, but in this same study Tambasco et al. [16] was found there was no influence on the maximum fractal dimension obtained.

Abu Eid & Landini [17] in 2003 quantified the global and local complexity of the interface tissue-conjunctival epithelium (CITEC) of 377 normal human oral mucosa, dysplastic and neoplastic diseases using digital images as tools and applying the Box-counting method for estimate the global fractal dimension and mass-radius to estimate the local fractal dimension. They found that CITEC has increased significantly from normal to pre-malignancy and

for this malignancy, both globally and locally. They concluded that fractal geometry is useful in assessing the changes of tissue complexity that occur due to malignant transformation by proposing the method as quantitative marker of epithelial complex.

Another advantage of the method, in our view, would be to provide a tool with the ability to bring consensus among pathologists in a relatively large number of cases of diagnostic uncertainty, thereby minimizing the intra- and interobserver variability. Moreover, it could also act as a screening method, identifying tumors of low and intermediate grades in high volume centers of motion, rationalizing the time spent by pathologists in the research areas of compromised tissue [16].

In this study we were able to differentiate the various degrees of rejection (1 versus zero, zero versus 2, 3 versus 0, 1 versus 2 and 3 versus 1). There was no possibility to differentiate between grades 3 and 2. The consensus among pathologists also could hardly be achieved in the current differentiation of 2 and 3 rejection grades, since the difference between them presents only available in inflammatory foci of grade 2, with two or more defined focus of aggression and the myocytes grade 3 with inflammatory infiltrate diffusely distributed with extensive destruction of fibers.

So this feature may not be enough to produce differences in the measurement of fractal dimension, raising the need for future studies with new approaches to complexity.

Regarding the study limitations that may be suggested, here are some counter-arguments:

a. The size of the boxes to calculate the fractal dimension in the Box-counting method was standardized at 4, 8, 16, 32 and 64 pixels. It is known that the pixel size depends on the degree of resolution used. As Tambasco et al. [16] stated, the size of the box used should have certain relation to the structure studied, because it can be so small that, in fact, there would be assessed the sub-components of the structure or so large that, in fact, there would be included in the measurement of components of structure area but not the structure of interest. These values, however, are the default values used in the literature and therefore probably not caused interference in the results.

b. Number of fragments collected at biopsy (three) could be considered small, as some authors recommend up to five or six, but the purpose of this study was not to diagnose the presence or absence of rejection but, compared to a specific finding of rejection, to assess whether there was association with a higher degree of fractal dimension.

CONCLUSIONS

1. It was found that the calculation of fractal dimension can contribute to the assessment of myocardial cellular rejection in patients undergoing endomyocardial biopsy after cardiac transplantation.

2. Higher degree of fractal dimension were directly associated with progressively larger myocardial cellular rejection.

3. These findings may help in decision making in doubtful clinical cases and those on which become known in the intensification of immunosuppressive medication.

ACKNOWLEDGEMENT

We thank Mr. Antonio Assad Mussi Koury, for the enormous contribution made in the graphical editing of histological images.

REFERENCES

1. Silva PR. Transplante cardíaco e cardiopulmonar: 100 anos de história e 40 de existência. Rev Bras Cir Cardiovasc. 2008;23(1):145-52.

2. Fiorelli AI, Abreu Filho CAC, Santos RHB, Buco FHA, Fiorelli LR, Bacal F, et al. Transplante cardíaco com anastomose bicaval e anuloplastia tricúspide profilática no enxerto. Rev Bras Cir Cardiovasc. 2008;23(1):7-13.

3. Barroso E, Garcia MI, Pinho JC, Guedes MV. Pós-operatório de transplante cardíaco e tratamento imunossupressor. Rev SOCERJ. 2002;15(3):164-71.

4. Morgun A, Shulzhenko N, Gerbase-DeLima M. Monitoração imunológica pós-transplante cardíaco. http://www.brazilpednews. org.br/junh2002/bnp06023.htm. Acesso em 01/11/2007.

5. Bacal F, Veiga VC, Fiorelli AI, Bellotti G, Bocchi EA, Stolf NAG, et al. Análise dos fatores de risco da doença vascular do enxerto em pacientes assintomáticos após transplante cardíaco. Arq Bras Cardiol. 2000;75(5):413-20.

6. Billingham ME, Cary NR, Hammond ME, Kemnitz J, Marboe C, McCallister HA, et al. A working formulation for the standardization of nomenclature in the diagnosis of heart and lung rejection: Heart Rejection Study Group. The International Society for Heart Transplantation. J Heart Transplant. 1990;9(6):587-93.

7. Rodriguez ER; International Society for Heart and Lung Transplantation. The pathology of heart transplant biopsy specimens: revisiting the 1990 ISHLT working formulation. J Heart Lung Transplant. 2003;22(1):3-15.

8. Karperien A, Jelinek HF, Leandro JJ, Soares JV, Cesar RM, Luckie A. Automated detection of proliferative retinopathy in clinical practice. Clin Ophthalmol. 2008;2(1):109-22.

9. Wielgus E, Pawlicki K, Kawa A, Wloch S, Kaminski M. Fractal analysis of placenta mature villi in healthy, smoking and non-smoking women. Med Sci Monit. 2000;6(2):271-7.

10. Dioguardi N, Grizzi F, Franceschini B, Bossi P, Russo C. Liver fibrosis and tissue architectural change measurement using fractal-rectified metrics and Hurst's exponent. World J Gastroenterol. 2006;12(14):2187-94.

11. Stewart S, Winters GL, Fishbein MC, Tazelaar HD, Kobashigawa J, Abrams J, et al. Revision of the 1990 working formulation for the standardization of nomenclature in the diagnosis of heart rejection. J Heart Lung Transplant. 2005;24(11):1710-20.

12. Benjamin JE, Gill S, Negrin RS. Biology and clinical effects of natural killer cells in allogeneic transplantation. Curr Opin Oncol. 2010;22(2):130-7.

13. Kido S, Ikezoe J, Naito H, Tamura S, Machi S. Fractal analysis of interstitial lung abnormalities in chest radiography. Radiographics. 1995;15(6):1457-64.

14. Vasilescu C, Herlea V, Taloº F, Ivanov B, Dobrescu R. Differences between intestinal and diffuse type of gastric carcinoma: a fractal analysis. http://isis.pub.ro/iafa2003/files/7-3.pdf Acesso em 28/6/2010.

15. Sullivan R, Holden T, Tremberger Jr E, Cheung E, Branch C, Burrero J, et al. Fractal dimension of breast cancer cell migration in a wound healing assay. Intern J Biological Life Sciences. 2010;6(3):170-5.

16. Tambasco M, Costello BM, Kouznetsov A, Yau A, Magliocco AM. Quantifying the architectural complexity of microscopic images of histology specimens. Micron. 2009;40(4):486-94.

17. Abu Eid R, Landini G. Quantification of the global and local complexity of the epithelial-connective tissue interface of normal, dysplastic, and neoplastic oral mucosae using digital imaging. Pathol Res Pract. 2003;199(7):475-82.